Dalton Transactions

Accepted Manuscript

This article can be cited before page numbers have been issued, to do this please use: L. Abad Galan, S. Wada, L. Cameron, A. N. Sobolev, Y. Hasegawa, E. Zysman-Colman, M. I. Ogden and M. Massi, *Dalton Trans.*, 2019, DOI: 10.1039/C8DT04749A.

ROYAL SOCIETY OF CHEMISTRY

rsc.li/dalton

ROYAL SOCIETY OF CHEMISTRY View Article Online
DOI: 10.1039/C8DT04749A

Journal Name

Received 00th January 20xx,
Accepted 00th January 20xx

DOI: 10.1039/x0xx00000x

www.rsc.org/

Photophysical investigation of near infrared emitting lanthanoid complexes incorporating tris(2-naphthoyl)methane as a new antenna ligand

Laura Abad Galán,[a],[b] Satoshi Wada,[c] Lee Cameron,[a] Alexandre N. Sobolev,[d] Yasuchika Hasegawa,[e] Eli Zysman-Colman,*[b] Mark I. Ogden,*[a] and Massimiliano Massi*[a]

A conjugated *β*-triketone, tris(2-naphthoyl)methane (**tnm**H), has been synthesized and successfully utilized as an antenna moiety for sensitization of the trivalent lanthanoids Eu^{3+}, Sm^{3+}, Yb^{3+} and Nd^{3+}, in an isomorphous series of mononuclear complexes formulated as $[Ln(\mathbf{tnm})_3(DMSO)_2]$ (Ln^{3+} = Nd^{3+}, Sm^{3+}, Eu^{3+}, Gd^{3+} and Yb^{3+}). The photophysical properties of the materials were characterized as comprehensively as possible, with overall quantum yields, intrinsic quantum yields based on calculated radiative decays, and sensitization efficiencies reported. This investigation improves understanding of the sensitization processes occurring in the near-infrared (NIR) region systems in particular, where quantitative data is currently scarce. In fact, the $[Yb(\mathbf{tnm})_3(DMSO)_2]$ and its deuterated analogue, $[Yb(\mathbf{tnm})_3(d_6\text{-}DMSO)_2]$, present high values of overall quantum yield of 4% and 6%, respectively, which makes them useful and readily accessible references for future investigation of NIR-emitting systems.

Introduction

The unique photophysical properties of the lanthanoid ions, such as characteristic line-like emission spectra and long luminescence lifetimes, have made them key elements in a range of technological applications.[1–4] Particular interest has been paid to the lanthanoids, Nd^{3+}, Er^{3+} and Yb^{3+}, exhibiting near infrared (NIR) emission because of their potential applications in biological imaging[4,5] and telecommunications.[6] To obtain highly efficient emissive lanthanoid complexes, their chemical nature must be carefully designed accounting for the nature of interconfigurational electronic *f-f* transitions. Indeed, *f-f* transitions are parity and often spin forbidden, and as such are characterized by low absorption coefficients. Therefore, an alternative sensitization pathway is required. The most common approach involves the use of organic ligands that are capable of harvesting light to be excited into their singlet manifold, which will consequently transfer energy to the lanthanoid excited states after intersystem crossing to the corresponding triplet excited state.[8,9] This sensitization mechanism is commonly known as the antenna effect. Different NIR luminescent lanthanoid complexes and materials have been developed over the past decades.[10–14] However, the overall quantum yields typically remain much lower[15] when compared to their analogous visible emitters.[16–18] The main reason for this behaviour is the facile quenching of the excited states of NIR emitters, particularly via multiphonon relaxation caused by high frequency vibration of OH, NH, and CH bonds in close proximity to the metal center.[14,19] Commonly explored strategies to increase the efficiency of NIR luminescence include perdeuteration or perfluorination of the coordinated ligands.[10,11,20–23] This strategy is effective as O-D and C-F bonds are less efficient in quenching lanthanoid excited states due to their lower stretching frequencies. The downside of this approach is the severe limitation imposed by perdeuteration or perfluorination on ligand design, availability and cost, including the fact that deuteration might not be a commonly available option in synthetic laboratories. More recently and less explored as a strategy, is the alteration of the donor atoms of

[a] School of Molecular and Life Sciences and Curtin Institute for Functional Molecules and Interfaces, Curtin University, Kent Street, Bentley 6102 WA, Australia.
[b] Organic Semiconductor Centre, EaStCHEM School of Chemistry, University of St. Andrews, St. Andrews, Fife, KY16 9ST, United Kingdom
[c] Graduate School of Chemical Sciences and Engineering, Hokkaido University, Kita-13 Jo, Nishi-8 Chome, Kita-ku, Sapporo, Hokkaido, 060-8628 Japan
[d] School of Molecular Sciences and CMCA, M310, University of Western Australia, Crawley 6009 WA, Australia.
[e] Faculty of Engineering, Hokkaido University, Kita-13 Jo, Nishi-8 Chome, Kita-ku, Sapporo, Hokkaido, 060-8628 Japan

*E-mail: m.massi@curtin.edu.au; m.ogden@curtin.edu.au; eli.zysman-colman@st-andrews.ac.uk

† Electronic Supplementary Information (ESI) available: NMR spectra and absorption profiles of the ligand; shape analysis, excitation, emission, and excited state lifetime decay plots, of the complexes. See DOI: 10.1039/x0xx00000x

the coordinated ligands in Yb^{3+} cryptates to increase the efficiency of NIR emission.[24] This particular design offers increased quantum yields by exploiting an increase of the radiative decay constant, k_r, in contrast to the reduction of the non-radiative decay constant, k_{nr}, obtained by perdeuteration or perfluorination of the ligands.

Recently, we have been interested in investigating the structural and photophysical properties of lanthanoid *β*-triketonate complexes. This investigation has been initiated by the lack of available data on these systems, whose ligands can be simply obtained *via* a Claisen condensation reaction of the well-known *β*-diketonate ligands, ubiquitous in lanthanoid chemistry. The peculiar feature observed for this system is the tendency to form tetranuclear complexes of the general formula $[LnAeL_4]_2$ (where Ln is a lanthanoid cation, Ae is a cationic alkaline elements, and L is a *β*-triketonate ligand), which can be either discrete complexes[25] or repeating units in monodimensional polymers.[26,27] In the case of Yb^{3+}, these assemblies displayed favourable NIR emission and were also found to be suitable as emitters in NIR-emitting organic light-emitting diodes.[28] Unfortunately, their poor solubility in organic solvents limited the depth of the photophysical investigation of these systems. To better understand the design rules required for improved NIR emission, the photophysical properties of a library of complexes of formulation $[Ln(\mathbf{tbm})_3(phen)]$ (Ln^{3+}= Eu^{3+}, Er^{3+} and Yb^{3+}; $\mathbf{tbm}^-$ = tribenzoylmethanide) was directly compared to those of $[Ln(\mathbf{dbm})_3(phen)]$ (Ln^{3+}= Eu^{3+}, Er^{3+} and Yb^{3+}; $\mathbf{dbm}^-$ = dibenzoylmethanide).[29] This study demonstrated only a small enhancement of the NIR emitting properties of the Yb^{3+} complexes, likely due to the removal of the α-CH bond on passing from $\mathbf{dbm}^-$ to $\mathbf{tbm}^-$. However, the photoluminescence lifetimes and quantum yields did not rival those found for the assemblies, which suggested that the NIR emission of the tetranuclear based complexes were most likely enhanced due to other factors related to their specific structure and composition.

In the present investigation, we have synthesised a new *β*-triketone bearing 2-naphthoyl substituents, tris(2-naphthoyl)methane (**tnm**H). The original idea was to investigate whether the 2-naphthoyl substituents would enhance the solubility of $[LnAeL_4]_2$ in organic solvents and favour the sensitization of the NIR lanthanoids by lowering the energy of the ligand triplet state upon increased conjugation with respect to $\mathbf{tbm}^-$. However, and despite multiple attempts, no such assembly structures could be obtained with the $\mathbf{tnm}^-$ ligand. On the other hand, a family of soluble mononuclear complexes with formula $[Ln(\mathbf{tnm})_3(DMSO)_2]$ (Ln^{3+}= Nd^{3+}, Sm^{3+}, Eu^{3+}, Gd^{3+} and Yb^{3+}) was isolated. The fact that these complexes are soluble allowed us to fully analyse their photophysical properties, including overall quantum yields, intrinsic quantum yields based on calculated radiative decays and sensitization efficiencies. Indeed, full quantitative characterization in the NIR is found to be scarce in the literature with only a limited set of examples reporting sensitization efficiencies. One of the most spectacular examples is a Yb^{3+} based molecular system using a perfluorinated porphyrin as the antenna and a tripodal Kläui co-ligand, which presents a sensitization efficiency of 100%.[23] However, there is a dearth of reports on the comprehensive photophysical characterization of *β*-diketonate containing complexes of Yb^{3+}. This makes comparison with other ligand moieties difficult and hinders the systematic development of these readily synthesized systems. In this report, we include full quantitative photophysical characterization, based on experimentally calculated radiative decays, which have been proven to range from 0.5 to 1.3 ms in solution.[8,30] In particular, $[Yb(\mathbf{tnm})_3(d_6\text{-DMSO})_2]$ possesses a lifetime of 40 µs, an intrinsic quantum yield of 6%, and a sensitization efficiency of 50%, thereby showing an improved photophysical behavior in comparison to our previously reported *β*-triketonate-based complex.[10,31,32] This complex has, to the best of our knowledge, optimal photophysical properties for Yb^{3+} *β*-diketonate-based coordination complexes including perfluorinated[31–34] and deuterated compounds.[10,21] Furthermore, this study shows how DMSO is a preferable ancillary ligand for NIR-mononuclear complexes in comparison to the commonly used 1,10-phenathroline, phen.

Experimental

General procedures

All reagents and solvents were purchased from chemical suppliers and used as received without further purification. Hydrated $LnCl_3$ precursors (Ln = Nd^{3+}, Sm^{3+}, Eu^{3+}, Gd^{3+}, Yb^{3+}) were prepared by the reaction of Ln_2O_3 with hydrochloric acid (5 M), followed by evaporation of the solvent under reduced pressure. Infrared spectra (IR) were recorded on solid-state samples using an attenuated total reflectance Perkin Elmer Spectrum 100 FT-IR. The spectra were recorded from 4000 to 650 cm^{-1}. The intensity of the IR bands is reported as strong (s), medium (m), or weak (w), with broad (br) bands also specified. Melting points were determined using a BI Barnsted Electrothermal 9100 apparatus. Elemental analyses were obtained using a Perkin Elmer PE 2400 CHN Elemental Analyser at Curtin University, Australia. Nuclear magnetic resonance (NMR) spectra were recorded using a Bruker Avance 400 spectrometer (400.1 MHz for ^1H; 100 MHz for ^{13}C) at 300 K. The data were acquired and processed by the Bruker TopSpin 3.1 software. All of the NMR spectra were calibrated to residual solvent signals.

Selected equations.

The values of the radiative lifetime (τ_R), and intrinsic quantum yield (Φ^{Ln}_{Ln}) can be calculated with the following equations.[36]

$$\frac{1}{\tau_R} = 14.65\ s^{-1} \times n^3 \times \frac{I_{Tot}}{I_{MD}} \qquad \text{(Eq. 1)}$$

In equation 1, the refractive index (n) of the solvent is used (assumed value of 1.5 in the solid state). The value 14.65 s^{-1} is the spontaneous emission probability of the $^7F_1 \leftarrow {}^5D_0$ transition reported previously.[35] I_{Tot} is the total integrated intensity of the Eu^{3+} emission spectrum, and I_{MD} is the integrated intensity of the $^7F_1 \leftarrow {}^5D_0$ band.

View Article Online
DOI: 10.1039/C8DT04749A

$$\frac{1}{\tau_r} = 2303\, x \frac{8\pi c n^2 \bar{\nu}^2 (2J+1)}{N_A (2J'+1)} \int \varepsilon(\check{\nu}) d\check{\nu} \qquad \text{(Eq. 2)}$$

In equation 2, N_A is Avogadro's number ($6.023x10^{23}$ mol^{-1}), whereas J and J' are the quantum numbers for the ground and excited state of Yb^{3+}, respectively.[30]

$$\Phi_{Ln}^{Ln} = \frac{\tau_{obs}}{\tau_R} \qquad \text{(Eq. 3)}$$

In equation 3, τ_{obs} is the observed lifetime.

Radiative and non-radiative constants can also be calculated from the radiative and observed lifetime decays, following equations 4 and 5.

$$\tau_{obs} = \frac{1}{k_r + k_{nr}} \qquad \text{(Eq. 4)}$$

$$\tau_r = \frac{1}{k_r} \qquad \text{(Eq. 5)}$$

Finally, the sensitization efficiency (η_{sens}) can be determined using equation 6, where Φ_{Ln}^{L} is the overall quantum yield obtained experimentally with an integrating sphere.

$$\eta_{sens} = \frac{\Phi_{Ln}^{L}}{\Phi_{Ln}^{Ln}} \qquad \text{(Eq. 6)}$$

Photophysical measurements

Absorption spectra were recorded at room temperature using a Perkin Elmer Lambda 35 UV/Vis spectrometer. Uncorrected steady state emission and excitation spectra were recorded using an Edinburgh FLSP980-stm spectrometer equipped with a 450 W xenon arc lamp, double excitation and emission monochromators, a Peltier cooled Hamamatsu R928P photomultiplier (185–850 nm) and a Hamamatsu R5509-42 photomultiplier for detection of NIR radiation (800-1400 nm). Emission and excitation spectra were corrected for source intensity (lamp and grating) and emission spectral response (detector and grating) by a calibration curve supplied with the instrument. Quantum yields were measured with the use of an integrating sphere coated with BenFlect.[47]

Excited-state decays (τ) were recorded on the same Edinburgh FLSP980-stm spectrometer using a microsecond flashlamp, set at excitation wavelength of 350 nm, and monitored at the maximum emission wavelength being 980 nm, 1080 nm, 612 nm and 645 nm for Yb^{3+}, Nd^{3+}, Eu^{3+} and Sm^{3+} complexes, respectively. The goodness of fit was assessed by minimizing the reduced χ^2 function and by visual inspection of the weighted residuals.

To record the luminescence spectra at 77 K, the samples were placed in quartz tubes (2 mm diameter) and inserted in a quartz Dewar filled with liquid nitrogen. All the solvents used in the preparation of the solutions for the photophysical investigations were of spectrometric grade.

Synthesis

Synthesis of di(2-naphthoyl)methane (dnmH)

The **dnm**H precursor was synthesized via Claisen condensation following a previously reported procedure.[36]

Synthesis of tris(2-naphthoyl)methane (tnmH)

2-Naphthoic acid (826 mg, 4.8 mmol) was added to thionyl chloride (5 mL, 25.6 mmol) and heated at reflux for 2 hours. After this time, the solvent was removed under reduced pressure and the remaining solid 2-naphthoyl chloride was immediately added to THF (20 mL). A suspension of NaH (60% in mineral oil, 72 mg, 3.6 mmol) in THF was prepared and maintained at 0 ºC. A 10 mL THF solution containing **dnm**H (389 mg, 1.2 mmol) was dropwise added and the mixture was stirred at 0 ºC for 30 minutes. To this suspension, the solution of 2-naphthalenecarbonyl chloride (686 mg, 3.6 mmol) in THF was added dropwise. After the addition, the mixture was stirred under nitrogen atmosphere at 40 ºC for 16 hours. The solvent was then removed under a reduced pressure and water (20 mL) was slowly added to the residual solid. The pH was adjusted to neutral after addition of an HCl solution (1 M). The aqueous phase was then extracted with ethyl acetate (3 x 15 mL). The combined organic layers were dried over $MgSO_4$. After removal of the solvent under reduced pressure, the targeted compound was isolated as a white solid. Yield 80%. M.p. 289- 291 °C. Elemental analysis calcd (%) for $C_{34}H_{22}O_3$: C, 85.34; H, 4.63; found: C, 84.91; H, 4.53. IR (ATR): ν = 3059 w, 1671 s, 1656 s, 1626 s, 1597 m, 1581 m, 1507 w, 1469 m, 1438 w, 1393 w, 1371 w, 1353 m, 1290 s, 1239 m, 1178 s, 1221 s, 1020 w, 1007 m, 947 m, 907 m, 860 m, 812 s, 764 w, 740 s. ^{1}H NMR (400 MHz, DMSO-d_6): δ 8.86 (s, 3H), 8.57 (s, 1H), 8.06 (dt (app. triplet), J = 14.3, 7.8 Hz, 12H), 7.71 (ddd, J = 8.2, 6.9, 1.2 Hz, 3H), 7.63 (ddd, J = 8.1, 7.0, 1.2 Hz, 3H) ppm. ^{13}C NMR (101 MHz, DMSO): δ 193.8, 135.4, 133.0, 132.1, 130.9, 129.8, 129.3, 128.8, 127.8, 127.3, 123.8, 65.5, 39.5 ppm.

General procedure for the synthesis of lanthanoid complexes

Triethylamine (3 equiv.) was added to a mixture containing **tnm**H (3 equiv.) and hydrated LnCl3 (ca. 20 mg) in DMSO (5 mL). The mixture was heated at 60°C for 30 minutes and then left at ambient temperature. After cooling to room temperature, a layer of EtOH was carefully added on top. Slow diffusion of the EtOH into the DMSO layer over several days afforded crystals suitable for X-ray diffraction.

[Nd(**tnm**)$_3$(DMSO)$_2$]: 50 mg (27%), M.p. 220-222 °C. Elemental analysis calcd (%) for $C_{106}H_{75}S_2O_{11}Nd$ (2·SOC_2H_6): C, 69.89; H, 4.45; found: C, 69.93; H, 4.64. IR (ATR): ν = 3053 w, 2918 w, 1619 w, 1596 m, 1539 s, 1505 w, 1375 s, 1308 m, 1242 w, 1204 w, 1112 m, 1020 m, 961 w, 909 m, 861 m, 819 s, 794 s, 757 m, 748 m, 730 m.

[Sm(**tnm**)$_3$(DMSO)$_2$]: 40 mg (12%), M.p. 214-216 °C. Elemental analysis calcd (%) for $C_{106}H_{75}S_2O_{11}Sm$ (2·SOC_2H_6): C, 70.52; H, 4.56; found: C, 70.83; H, 4.56. IR (ATR): ν = 3054 w, 1622 w, 1540 s, 1505 w, 1465 w, 1433 w, 1373 s, 1333 m, 1242

w, 1151 w, 1112 m, 1020 m, 962 w, 907 m, 862 w, 819 m, 793 m, 756 w, 730 w, 508 w, 476 m.

[Eu(**tnm**)$_3$(DMSO)$_2$]: 65 mg (27%), M.p. 210-212 °C. Elemental analysis calcd (%) for $C_{106}H_{75}S_2O_{11}Eu$ (2· SOC_2H_6): C, 69.64; H, 4.62; found: C, 70.02; H, 4.38. IR (ATR): ν = 3054 w, 1623 m, 1576 m, 1543 s, 1465 m, 1433 m, 1372 s, 1333 s, 1309 s, 1242 m, 1204 w, 1151 m, 1111 m, 1023 m, 962 m, 906 m, 863 m, 818 m, 793 s, 756 m, 731 m.

[Gd(**tnm**)$_3$(DMSO)$_2$]: 58 mg (32%), M.p. 204-206 °C. Elemental analysis calcd (%) for $C_{106}H_{75}S_2O_{11}Gd$ (4· SOC_2H_6): C, 66.51; H, 4.854; found: C, 66.81; H, 4.60. IR (ATR): ν = 3053 w, 1624m, 1577 m, 1543 s, 1505 w, 1466 w, 1433 w, 1374 s, 1335 s, 1301 s, 1242 m, 1204 w, 1112 m, 1020 m, 961 m, 863 m, 818 s, 792 s, 763 m, 731 m.

[Yb(**tnm**)$_3$(DMSO)$_2$]: 68 mg (37%), M.p. 186-188 °C. Elemental analysis calcd (%) for $C_{106}H_{75}S_2O_{11}Yb$ (2.5· SOC_2H_6): C, 68.12; H, 4.63; found: C, 68.44; H, 4.28. IR (ATR): ν = 3054 w, 1625 m, 1597 m, 1578 m, 1547s, 1505 w, 1466 w, 1434 w, 1376 s, 1336 s, 1302 s, 1243 m, 1152 w, 1112 m, 1022 m, 961 w, 906 m, 863 w, 818 s, 792 s, 763 m, 732 m.

Crystallography

Crystallographic data for the structures were collected at 100(2) K on an Oxford Diffraction Gemini or Xcalibur diffractometer fitted with Mo-Kα or Cu-Kα radiation**.** Following Lp and absorption corrections and solution by direct methods, the structures were refined against F^2 with full-matrix least-squares using the program SHELX-2014.[37]

Anisotropic displacement parameters were employed for the non-hydrogen atoms. All hydrogen atoms were added at calculated positions and refined by use of a riding model with isotropic displacement parameters based on those of the parent atom. The complete crystallographic data for the structures reported in this paper have been deposited at the Cambridge Crystallographic Data Centre with supplementary publication numbers given below. Copies of the data can be obtained free of charge *via* https://www.ccdc.cam.ac.uk/structures/, or from the Cambridge Crystallographic Data Centre, 12 Union Road, Cambridge CB2 1EZ, U.K.; fax: (+44) 1223-336-033; or e-mail: data_request@ccdc.cam.ac.uk

X-ray data refinement

[Nd(**tnm**)$_3$(DMSO)$_2$]: 2($C_{106}H_{75}O_{11}S_2Nd$), C_2H_6OS, 1.5(C_2H_6O, H_2O) M = 3640.28, pale yellow plate, 0.416 × 0.200 × 0.070 mm^3, triclinic, space group P-1 (No. 2), a = 13.2128(4), b = 17.3769(4), c = 20.8146(4) Å, α = 89.837(2), β = 75.481(2), γ = 85.908(2)°, V = 4614.0(2) Å^3, Z = 1, D_c = 1.310 g cm^{-3}, μ = 0.683 mm^{-1}. F_{000} = 1878, MoKα radiation, λ = 0.71073 Å, T = 100(2) K, $2\theta_{max}$ = 64.7°, 100011 reflections collected, 30417 unique (R_{int} = 0.0583). Final *GooF* = 1.002, R1 = 0.0561, wR2 = 0.1389, R indices based on 23101 reflections with $I > 2\sigma(I)$ (refinement on F^2), $|\Delta\rho|_{max}$= 1.1(1) e Å^{-3}, 1446 parameters, 378 restraints. CCDC 1876760

[Sm(**tnm**)$_3$(DMSO)$_2$]: 2($C_{106}H_{75}O_{11}S_2$ Sm), C_2H_6OS, 1.5(C_2H_6O, H_2O), M = 3652.50, pale yellow plate, 0.273 × 0.192 × 0.059 mm^3, triclinic, space group P-1 (No. 2), a = 13.2079(4), b = 17.3573(5), c = 20.7486(6) Å, α = 89.751(2), β = 75.806(3), γ = 85.757(2)°, V = 4598.4(2) Å^3, Z = 1, D_c = 1.319 g cm^{-3}, μ = 0.759 mm^{-1}. F_{000} = 1882, MoKα radiation, λ = 0.71073 Å, T = 100(2) K, $2\theta_{max}$ = 64.8°, 96497 reflections collected, 30304 unique (R_{int} = 0.0599). Final *GooF* = 1.001, R1 = 0.0533, wR2 = 0.1214, R indices based on 23713 reflections with $I > 2\sigma(I)$ (refinement on F^2), $|\Delta\rho|_{max}$= 1.9(1) e Å^{-3}, 1446 parameters, 378 restraints. CCDC 1876762

[Eu(**tnm**)$_3$(DMSO)$_2$]: 2($C_{106}H_{75}O_{11}S_2Eu$), C_2H_6OS, 1.5(C_2H_6O, H_2O), M = 3655.72, pale yellow plate, 0.26 × 0.22 × 0.04 mm^3, triclinic, space group P-1 (No. 2), a = 13.2024(3), b = 17.3493(4), c = 20.7471(5) Å, α = 89.687(2), β = 75.677(2), γ = 85.672(2)°, V = 4590.90(19) Å^3, Z = 1, D_c = 1.322 g/cm^3, μ = 5.933 mm^{-1}. F_{000} = 1884, CuKα radiation, λ = 1.54178 Å, T = 100(2)K, $2\theta_{max}$ = 134.7º, 46811 reflections collected, 16278 unique (R_{int} = 0.0426). Final *GooF* = 1.005, *R1* = 0.0411, *wR2* = 0.1068, R indices based on 14775 reflections with I > 2σ(*I*) (refinement on F^2), $|\Delta\rho|_{max}$= 0.77(7) e Å^{-3}, 1444 parameters, 360 restraints. CCDC 1876758

[Gd(**tnm**)$_3$(DMSO)$_2$]: 2($C_{106}H_{75}O_{11}S_2Gd$) , C_2H_6OS, 1.5(C_2H_6O, H_2O), M = 3666.30, pale yellow plate, 0.166 × 0.102 × 0.021 mm^3, triclinic, space group P-1 (No. 2), a = 13.2123(4), b = 17.3707(5), c = 20.7312(5) Å, α = 89.738(2), β = 75.704(2), γ = 85.603(2)°, V = 4596.5(2) Å^3, Z = 1, D_c = 1.324 g cm^{-3}, μ = 5.708 mm^{-1}. F_{000} = 1886, CuKα radiation, λ = 1.54178 Å, T = 100(2) K, $2\theta_{max}$ = 133.2º, 126377 reflections collected, 16220 unique (R_{int} = 0.1306). Final *GooF* = 1.000, R1 = 0.0516, wR2 = 0.1237, R indices based on 12817 reflections with $I > 2\sigma(I)$ (refinement on F^2), $|\Delta\rho|_{max}$= 0.83(8) e Å^{-3}, 1446 parameters, 366 restraints. CCDC 1876759

[Yb(**tnm**)$_3$(DMSO)$_2$]: 2($C_{106}H_{75}O_{11}S_2Yb$), C_2H_6OS, 1.5(C_2H_6O, H_2O), M = 3697.88, pale yellow plate, 0.322 × 0.248 × 0.074 mm^3, triclinic, space group P-1 (No. 2), a = 13.2004(3), b = 17.3176(4), c = 20.6645(5) Å, α = 89.505(2), β = 75.711(2), γ = 85.494(2)°, V = 4563.32(19) Å^3, Z = 1, D_c = 1.346 g cm^{-3}, μ = 1.146 mm^{-1}. F_{000} = 1898, MoKα radiation, λ = 0.71073 Å, T = 100(2) K, $2\theta_{max}$ = 64.7º, 98398 reflections collected, 29997 unique (R_{int} = 0.0548). Final *GooF* = 1.003, R1 = 0.0568, wR2 = 0.1451, R indices based on 25610 reflections with $I > 2\sigma(I)$ (refinement on F^2), $|\Delta\rho|_{max}$= 2.1(1) e Å^{-3}, 1446 parameters, 366 restraints. CCDC 1876761

[Yb(**tnm**)$_3$(d_6-DMSO)$_2$]: 2($C_{106}H_{63}D_{12}O_{11}S_2Yb$), C_2D_6OS, 1.5(C_2H_6O, H_2O), M = 3728.07, pale yellow plate, 0.268 × 0.253 × 0.058 mm^3, triclinic, space group P-1 (No. 2), a = 13.1851(2), b = 17.3108(3), c = 20.6431(3) Å, α = 89.460(1), β = 75.870(1), γ = 85.536(1)°, V = 4555.04(13) Å^3, Z = 1, D_c = 1.359 g cm^{-3}, μ = 1.148 mm^{-1}. F_{000} = 1898, MoKα radiation, λ = 0.71073 Å, T = 100(2) K, $2\theta_{max}$ = 64.6°, 95688 reflections collected, 29877 unique (R_{int} = 0.0437). Final *GooF* = 1.000, R1 = 0.0454, wR2 = 0.1185, R indices based on 25872 reflections with $I > 2\sigma(I)$ (refinement on F^2), $|\Delta\rho|_{max}$= 2.4(1) e Å^{-3}, 1446 parameters, 366 restraints. CCDC 1876763

View Article Online
DOI: 10.1039/C8DT04749A

Results and discussion

Synthesis of the lanthanoid complexes.

The **tnm**H ligand was synthesized following a similar procedure to that previously reported for analogous *β*-triketones.[26,28] Given our previous study highlighting retro-Claisen reactivity for *β*-triketonates,[38] the stability of **tnm**H in deuterated DMSO (*ca*. 10^{-2} M) and in the presence of one equivalent of KOH was verified by ^{1}H-NMR. The sequential spectra showed no change in the resonances belonging to **tnm**H and no appearance of new resonances over 5 days thereby confirming the stability of this ligand under the complexation conditions (see supplementary information).

Three equivalents of **tnm**H and three equivalents of KOH were made to react with one equivalent of hydrated $LnCl_3$ (Ln^{3+}= Nd^{3+}, Sm^{3+}, Eu^{3+}, Gd^{3+}, Yb^{3+}) in DMSO. Single crystals suitable for X-ray diffraction were collected by slow diffusion of ethanol into the DMSO solution, with moderate yields of around 30%. Elemental analyses suggest the formation of monomeric species with formula [Ln(**tnm**)$_3$(DMSO)$_2$] for all the trialled lanthanoid cations (with variable degree of solvation), which were consistent with the X-ray structure determinations. The complexes display octacoordinated Ln^{3+} centers surrounded by six O-keto atoms from three **tnm**$^-$ ligands and two O atoms from two coordinated DMSO molecules. Overall, the eight O atoms from the ligands are arranged into a slightly distorted triangular dodecahedron (Figure 1). Intermolecular interactions are found between the uncoordinated keto O(22,32) atoms and methyl groups of DMSO molecules bound to neighbouring lanthanoid centers (O22….C1, 3.019Å; O32…C4, 3.187Å).

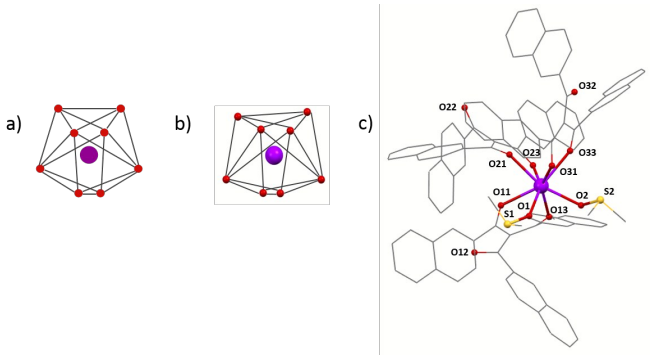

Figure 1. Representation of an ideal triangular dodecahedron (a), coordination environment for the Eu^{3+} cation in [Eu(**tnm**)$_3$(DMSO)$_2$] (b) and crystal structure of the [Eu(**tnm**)$_3$(DMSO)$_2$] coordination complex with H atoms omitted for clarity (c).

Table 1. Maximum and minimum Ln-O bond length (Å) for the [Ln(**tnm**)$_3$(DMSO)$_2$] complexes.

Complex	Ln-O (Å)
[Nd(**tnm**)$_3$(DMSO)$_2$]	2.464(2)- 2.377(2)
[Sm(**tnm**)$_3$(DMSO)$_2$]	2.436(2)-2.360(2)
[Eu(**tnm**)$_3$(DMSO)$_2$]	2.431(2)- 2.344(2)
[Gd(**tnm**)$_3$(DMSO)$_2$]	2.420(3)- 2.325(3)
[Yb(**tnm**)$_3$(DMSO)$_2$]	2.369(3)- 2.265(2)

Photophysical investigation

The photophysical data, which include excited state lifetime decay (τ_{obs}), calculated radiative decay (τ_R), intrinsic photoluminescence quantum yield (Φ_{Ln}^{Ln}), overall photoluminescence quantum yield (Φ_{Ln}^{L}), and calculated sensitization efficiency (η_{sens}), for Eu^{3+} and Yb^{3+} are reported in Table 2, while associated data for the relatedSm^{3+} and Nd^{3+} complexes can be found in the supplementary information.

The energy of the lowest singlet (25,907 cm^{-1}) and triplet excited state (19,250 cm^{-1}) of the **tnm**$^-$ ligand were estimated at the 0-phonon transition of the emission band originating from the [Gd(**tnm**)$_3$(DMSO)$_2$] complex in a frozen acetonitrile matrix (see supporting information). The energy of the triplet state is the lowest found for the family of *β*-triketonates molecules investigated to date, which is ascribed to the increased π-conjugation within the naphthyl substituents. The triplet excited state of **tnm**$^-$ should be able to promote sensitized near-infrared emission for the Yb^{3+} and Nd^{3+} complexes. The energy gap between the triplet excited state of **tnm**$^-$ and the accepting states of Eu^{3+} ($^5D_1$ ~19,000 cm^{-1} and $^5D_0$ ~17,200 cm^{-1})[39] and Sm^{3+} ($^4G_{5/2}$ ~18,000 cm^{-1}) is lower than 3,500 cm^{-1} and, therefore back energy transfer might be expected to some extent at room temperature.[40] In each case, the lanthanoid-centered emission of the complexes appears to be the result of the antenna effect, as broad excitation spectra analogous to the absorption profiles of the **tnm**$^-$ ligand are observed (see supporting information).

*[Yb(**tnm**)$_3$(DMSO)$_2$]*

Characteristic Yb^{3+} NIR centered emission was observed in the 900-1100 nm region from the [Yb(**tnm**)$_3$(DMSO)$_2$] acetonitrile solution at room temperature, 77 K, and solid state (Figure 2). The band corresponding to the spin allowed $^2F_{7/2}\leftarrow{}^2F_{5/2}$ transition is split into four peaks, consistent with Kramer's degeneracy, with the two lower energy peaks being quasi-degenerate due to crystal field effects. A shoulder in the 930-960 nm region is visible from measurements in solution and solid state at room temperature, which is ascribed to emission from hot excited states. This conclusion is corroborated by the fact that this shoulder is absent in the emission spectrum measured at 77 K. In all three cases, the excited lifetime decays were fitted to monoexponential functions. The overall quantum yields in solution were calculated relative to a toluene solution of [Yb(**tta**)$_3$(phen)] (**tta** = thenoyltrifluoroacetonato; phen = 1,10-phenanthroline), used as a standard. The overall quantum yields in the solid state were measured following a previously reported procedure with the use of an integrating sphere and two different detectors (visible and NIR).[29]

View Article Online
DOI: 10.1039/C8DT04749A

Table 2. Photophysical data for the complexes in the solid state, acetonitrile solution (*ca.* 10^{-5} M) and frozen matrix.

Complex	Media	τ_{obs}(μs)[a]	τ_R(ms)	Φ^{Ln}_{Ln}(%)	Φ^{L}_{Ln}(%)	η_{sens}(%)
[Yb(**tnm**)$_3$(DMSO)$_2$]	MeCN (RT)	39	0.53	7.4	3.6 [a]	49
	MeCN (77K)	44	-	-	-	-
	Solid State	18	-	-	4.2 [b]	-
[Yb(**tnm**)$_3$(d_6-DMSO)$_2$]	MeCN (RT)	40	-	-	3.1 [a]	-
	MeCN (77K)	50	-	-	-	-
	Solid State	35	-	-	6.1 [b]	-
[Eu(**tnm**)$_3$(DMSO)$_2$]	MeCN (RT)	20	1.37	1.4	0.2 [a]	14
	MeCN (77K)	394	0.88	45	-	-
	Solid State	117	1.48	7.9	0.7 [b]	9

[a] Quantum yield relative to a solution of [Yb(tta)$_3$(phen)] (phen = 1,10-phenanthroline; tta = thenoyltrifluoroacetonato) in toluene (Φ^{L}_{Ln}=1.6%).[10]
[b] Measured with the use of an integrating sphere.

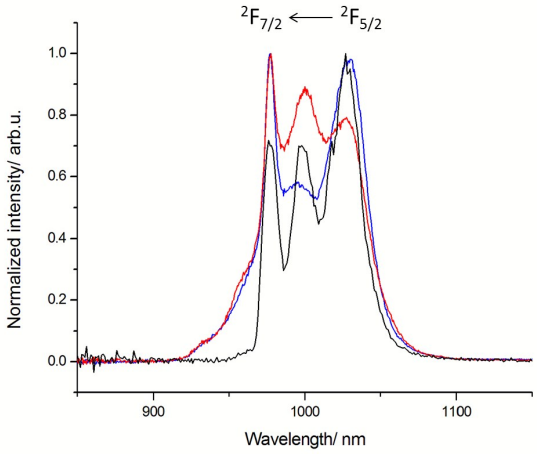

Figure 2. Normalized emission plots [Yb(**tnm**)$_3$(DMSO)$_2$] in the solid state (red trace), MeCN at RT (blue trace) and 77K (black trace), with excitation wavelength at 350 nm.

In the case of acetonitrile at room temperature, the observed excited state lifetime decay was found to be 39 μs and the overall quantum yield was 3.6%. The radiative decay was calculated from the absorption band corresponding to the direct excitation of the Yb^{3+} center (Figure 3). Following a modified Einstein equation (Eq. 2), the radiative decay was calculated to be 0.53 ms, which is comparable to previous reports in the literature,[30] but much shorter than the standard assumption of 1.2 ms for Yb^{3+} complexes in solution.[8] This is not surprising, as radiative lifetimes are known to vary significantly, depending on the coordination environment and identity of the donor atoms in the coordinating ligands.[15,24] The intrinsic quantum yield was then calculated (7.4%) giving a sensitization efficiency of 49%. These values are higher than our previously published mononuclear *β*-triketonate based complex [Yb(**tbm**)$_3$(phen)] (τ_{obs} = 18 μs and Φ^{L}_{Ln} = 1.16%)[29] and non-deuterated *β*-diketonate based systems[10,31,41–43]. In order to better understand the reason for such an improvement, the radiative decay of the previously reported [Yb(**tbm**)$_3$(phen)] was also determined to be 0.78 ms following the same methodology (Figure 3). This value was found to be longer than the radiative decay of [Yb(**tnm**)$_3$(DMSO)$_2$] (τ_R= 0.53 ms) where the two molecules of DMSO complete the coordination sphere with two O donor atoms instead of the two N atoms of phen. These results are consistent with those found in the literature where the radiative decay of Yb^{3+}-based cryptates was shortened when chelating via 2,2'-bipyridine-N,N'-dioxide ($bpyO_2$) instead of 2,2'-bipyridine (bpy).[24] With the value of the radiative lifetime in hand, the intrinsic quantum yield was calculated to be 2.3%, giving a sensitization efficiency of 50% and indicating analogous antenna effects from the **tnm**$^-$ and **tbm**$^-$ towards Yb^{3+}. On the other hand, the magnitude of the non-radiative decay constant (k_{nr}) for both complexes, [Yb(**tnm**)$_3$(DMSO)$_2$] (k_{nr}= $2.37{\cdot}10^4$ s^{-1}) and [Yb(**tbm**)$_3$(phen)] (k_{nr}= $5.43{\cdot}10^4$ s^{-1}), suggests that the higher value of intrinsic quantum yields for [Yb(**tnm**)$_3$(DMSO)$_2$] is due to a combination of less efficient non-radiative pathways occurring in the case of the DMSO complex and with a shorter radiative decay constant. To further validate this hypothesis, the analogous deuterated [Yb(**tnm**)$_3$(d_6-DMSO)$_2$] was investigated. As can be seen comparing the data in Table 2 for the two complexes coordinated to non-deuterated and deuterated DMSO, the excited state lifetime decay and overall quantum yield values are virtually the same when factoring in instrumental uncertainties. Given the ease of coordination of DMSO, these data suggest that to obtain efficient Yb^{3+} emitters the choice of this solvent to complete the coordination sphere is better than a conjugated chelating ligand with N atoms as donors such as phen as the latter contains with C-H bonds in closer proximity to the Yb^{3+} center.

View Article Online
DOI: 10.1039/C8DT04749A

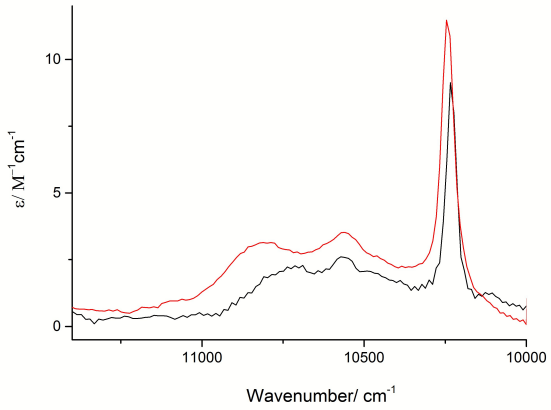

Figure 3. Absorption spectrum of [Yb(**tnm**)$_3$(DMSO)$_2$] *ca.* 6.24·10^{-4} M in acetonitrile (red trace) and [Yb(**tbm**)$_3$(phen)] *ca.* 1.57·10^{-3} M in dichloromethane (black trace).

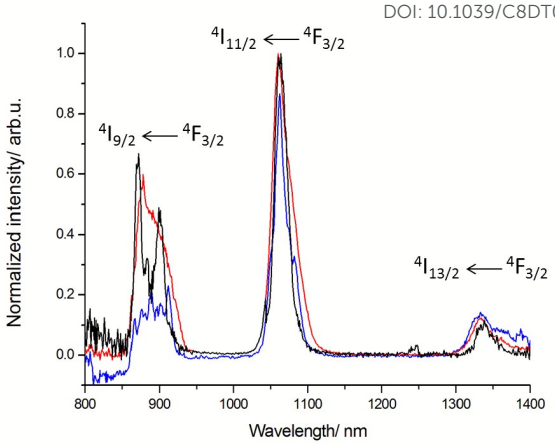

Figure 4. Normalized emission plots [Nd(**tnm**)$_3$(DMSO)$_2$] in the solid state (red trace), MeCN at RT (blue trace) and 77K (black trace), with excitation wavelength at 350 nm.

When the excited state lifetime decays were measured in a frozen matrix for [Yb(**tnm**)$_3$(DMSO)$_2$] and [Yb(**tnm**)$_3$(d_6-DMSO)$_2$], only a slight elongation was found in both cases and in agreement with the fact that no thermally activated backtransfer is accessible from the $^2F_{5/2}$ excited state of Yb^{3+}.
In the solid state, [Yb(**tnm**)$_3$(DMSO)$_2$] and [Yb(**tnm**)$_3$(d_6-DMSO)$_2$] are found to be isomorphous as determined via single crystal X-ray diffraction. The excited state lifetime decay and quantum yield of the complex bound to deuterated DMSO appear to be slightly higher that the non-deuterated complex, potentially suggesting quenching pathways from lattice solvent molecules.

*[Nd(**tnm**)$_3$(DMSO)$_2$]*
The Nd^{3+} complex displays characteristic emission peaks that are attributed to the $^7I_J \leftarrow {}^4F_{3/2}$ (J= 9/2, 11/2, 13/2) transition in the 900-1400 region (Figure 4) The structure and splitting of the bands is a consequence of the crystal field effects. The excited lifetime decay was found to be monoexponential in both media after deconvolution from instrumental response. The values of overall quantum yields were recorded in a similar manner to the Yb^{3+} complex.
In this case the photophysical data is comparable in both systems with lifetimes of 10 µs and 11 µs and overall quantum yields of 0.4% and 1.2% for the acetonitrile solution and solid state, respectively. The emission bands at 77K, are visibly more structured and the lifetime decay (10 µs) is comparable to the room temperature value.

*[Eu(**tnm**)$_3$(DMSO)$_2$]*
The emission spectra of [Eu(**tnm**)$_3$(DMSO)$_2$] in the three different media show the characteristic Eu^{3+} line-like bands attributed to the $^7F_J \leftarrow {}^5D_0$ (J= 0-4) transition in the region 550-750 nm (Figure 5). The $^7F_0 \leftarrow {}^5D_0$ peak appears narrow for the solid state and frozen matrix (~35 cm^{-1}) suggestive of the presence of a unique Eu^{3+} site.[35] The peak appears broader in acetonitrile solution at room temperature (~70 cm^{-1}), which is ascribed to the higher degree of freedom and the flexible coordination geometry of lanthanoid cations. The slightly different splitting of the $^7F_1 \leftarrow {}^5D_0$ and the $^7F_2 \leftarrow {}^5D_0$ bands suggests different degrees of distortion between the different media. In the three cases, the excited lifetime decays were satisfactorily fitted to monoexponential functions.
In the case of the acetonitrile solution at room temperature, the values of observed lifetime and radiative decay were found to be 20 µs and 1.37 ms, respectively, giving an intrinsic quantum yield of 1.4%. The short lifetime value and low quantum yield values suggest efficient quenching of the $^5D_0$ excited state, which might be ascribed to back energy transfer. This explanation is also supported by the very low value of the overall quantum yield (0.24%), thus resulting in a poor sensitization efficiency of 14%. When the same measurements were performed in the solid state the emission lifetime (117 µs), intrinsic quantum yield (7.9%) and overall quantum yield (0.7%) suggest that back energy transfer is also occurring here as well. To support our conclusion, the measurements were performed at 77 K, where back energy transfer is unlikely to occur, and the observed lifetime decay increased to 394 µs with an intrinsic quantum yield of 45%.

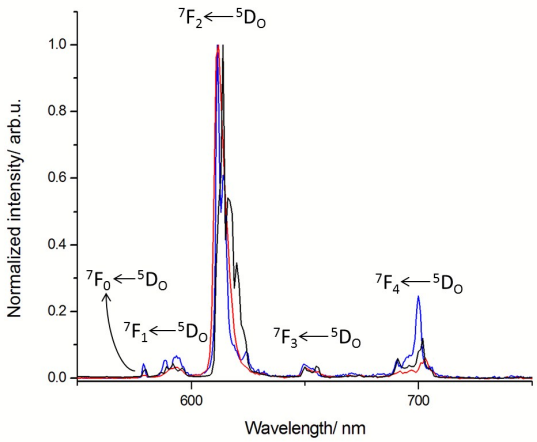

Figure 5. Normalized emission plots [Eu(**tnm**)$_3$(DMSO)$_2$] in the solid state (red trace), MeCN at RT (blue trace) and 77K (black trace), with excitation wavelength at 350 nm.

*[Sm(**tnm**)$_3$(DMSO)$_2$]*

The emission spectrum of the Sm^{3+} complex in the three media showed the characteristic $^6H_J \leftarrow {}^4G_{5/2}$ (J= 5/2, 7/2, 9/2 and 11/2) transitions in the region 550-750 nm (Figure 6). However, ligand emission is also observed in the case of the acetonitrile solution at room temperature as expected from poor sensitization due to back energy transfer (BET) from the triplet state of the ligand to the $^4G_{5/2}$ of Sm^{3+}. This is supported by the results found at 77K, where suppression of the ligand emission is observed by restriction of BET. The values of observable lifetime were found to be 7.74 µs, 9.34 µs and 142 µs in the solid state, room temperature acetonitrile and glassy acetonitrile, respectively. The elongation of the lifetime found at 77K further confirms the restriction of BET.

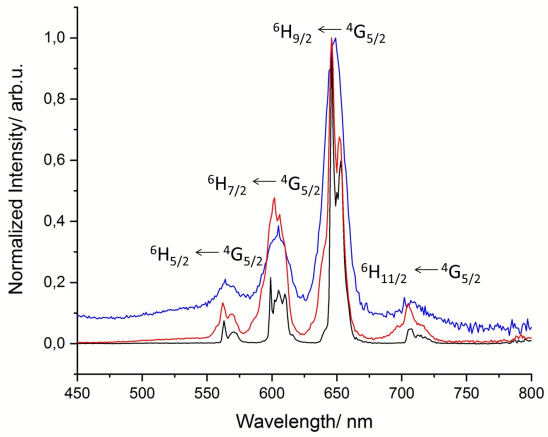

Figure 6. Normalized emission plots [Sm(**tnm**)$_3$(DMSO)$_2$] in the solid state (red trace), MeCN at RT (blue trace) and 77K (black trace), with excitation wavelength at 350 nm.

Conclusions

A synthetic pathway to make soluble and stable *β*-triketonate-based complexes has been reported, resulting in a new family of mononuclear complexes with formula [Ln(**tnm**)$_3$(DMSO)$_2$] for Ln^{3+} = Nd^{3+}, Sm^{3+}, Eu^{3+}, Gd^{3+} and Yb^{3+}. The full photophysical characterisation of the Yb-emitting complexes, has allowed us to determine that DMSO acts as a potentially better ancillary ligand than the often utilized phen, as it seems to reduce non-radiative decay pathways. In particular, [Yb(**tnm**)$_3$(d_6-DMSO)$_2$] presents a sensitization efficiency of 50% with a relatively high overall quantum yield of 6%, which are improved photophysical properties in comparison to their *β*-diketonate analogues.

Conflicts of interest

There are no conflicts to declare.

Acknowledgements

This research was partially supported by the Australian Research Council's Discovery *Projects* funding scheme (project DP17010189), and a Royal Society International Exchanges Grant. EZ-C thanks EPSRC (EP/M02105X/1) for support. L.A.G thanks Curtin University for the postgraduate scholarship.

Notes and references

1 J.-C. G. Bünzli and C. Piguet, *Chem. Soc. Rev.*, 2005, **34**, 1048–1077.
2 S. V. Eliseeva and J.-C. G. Bünzli, *Chem. Soc. Rev.*, 2010, **39**, 189–227.
3 J.-L. Liu, Y.-C. Chen and M.-L. Tong, *Chem. Soc. Rev.*, 2018, **47**, 2431–2453.
4 J. W. Walton, A. Bourdolle, S. J. Butler, M. Soulie, M. Delbianco, B. K. McMahon, R. Pal, H. Puschmann, J. M. Zwier, L. Lamarque, O. Maury, C. Andraud and D. Parker, *Chem. Commun.*, 2013, **49**, 1600–1602.
5 J.-C. G. Bünzli, *Luminescence Bioimaging with Lanthanide Complexes*, In *Luminescence of Lanthanide Ions in Coordination Compounds and Nanomaterials*, A. de Bettencourt-Dias (Ed.), John Wiley & Sons, Chichester, 2014, ch. 4, 125-196.
6 J.-C. G. Bünzli and S. V. Eliseeva, *J. Rare Earths*, 2010, **28**, 824–842.
7 S. Comby and J. C. G. Bünzli, *Handb. Phys. Chem. Rare Earths*, 2007, **37**, 217–470.
8 J. G. Bunzli and S. V Eliseeva, *Springer Ser. Fluoresc.*, 2011, 1–45.
9 S. Cotton, *Lanthanide and Actinide Chemistry*, John Wiley & Sons, Ltd, Chichester, UK, 2005.
10 M. P. Tsvirko, S. B. Meshkova, V. Y. Venchikov, Z. M. Topilova and D. V. Bol'shoi, *Opt. Spectrosc.*, 2001, **90**, 669–673.
11 A. W. Woodward, A. Frazer, A. R. Morales, J. Yu, A. F. Moore, A. D. Campiglia, E. V. Jucov, T. V. Timofeeva and K. D. Belfield, *Dalt. Trans.*, 2014, **43**, 16626–16639.
12 X. Guo, H. Guo, L. Fu, L. D. Carlos, R. A. S. Ferreira, L. Sun, R. Deng and H. Zhang, *J. Phys. Chem. C*, 2009, **113**, 12538–12545.
13 C. Yu, Z. Zhang, L. Liu, W. Feng, X. Lü, W. K. Wong and R. A. Jones, *Inorg. Chem. Commun.*, 2014, **49**, 30–33.
14 E. R. Trivedi, S. V. Eliseeva, J. Jankolovits, M. M. Olmstead, S. Petoud and V. L. Pecoraro, *J. Am. Chem. Soc.*, 2014, **136**, 1526–1534.
15 N. M. Shavaleev, S. V Eliseeva, R. Scopelliti and J. G. Bunzli, *Inorg. Chem.*, 2015, **54**, 9166–9173.
16 O. L. Malta, H. F. Brito, J. F. S. Menezes, F. R. G. E. Silva, C. D. Donega and S. Alves, *Chem. Phys. Lett.*, 1998, **282**, 233–238.

View Article Online
DOI: 10.1039/C8DT04749A

17 O. Moudam, B. C. Rowan, M. Alamiry, P. Richardson, B. S. Richards, A. C. Jones and N. Robertson, *Chem. Commun.*, 2009, **43**, 6649–6651.
18 C. Wei, B. Sun, Z. Cai, Z. Zhao, Y. Tan, W. Yan, H. Wei, Z. Liu, Z. Bian and C. Huang, *Inorg. Chem.*, 2018, **57**, 7512–7515.
19 A. P. Bassett, R. Van Deun, P. Nockemann, P. B. Glover, B. M. Kariuki, K. Van Hecke, L. Van Meervelt and Z. Pikramenou, *Inorg. Chem.*, 2005, **44**, 6140–6142.
20 P. B. Glover, A. P. Bassett, P. Nockemann, B. M. Kariuki, R. Van Deun and Z. Pikramenou, *Chem. - A Eur. J.*, 2007, **13**, 6308–6320.
21 R. H. C. Tan, M. Motevalli, I. Abrahams, P. B. Wyatt and W. P. Gillin, *J. Phys. Chem. B*, 2006, **110**, 24476–24479.
22 W. Wu, X. Zhang, A. Y. Kornienko, G. A. Kumar, D. Yu, T. J. Emge, R. E. Riman and J. G. Brennan, *Inorg. Chem.*, 2018, **57**, 1912–1918.
23 J. Y. Hu, Y. Ning, Y. S. Meng, J. Zhang, Z. Y. Wu, S. Gao and J. L. Zhang, *Chem. Sci.*, 2017, **8**, 2702–2709.
24 C. Doffek and M. Seitz, *Angew. Chemie - Int. Ed.*, 2015, **54**, 9719–9721.
25 B. L. Reid, S. Stagni, J. M. Malicka, M. Cocchi, A. N. Sobolev, B. W. Skelton, E. G. Moore, G. S. Hanan, M. I. Ogden and M. Massi, *Chem. - A Eur. J.*, 2015, **21**, 18354–18363.
26 L. Abad Galán, B. L. Reid, S. Stagni, A. N. Sobolev, B. W. Skelton, M. Cocchi, J. M. Malicka, E. Zysman-Colman, E. G. Moore, M. I. Ogden and M. Massi, *Inorg. Chem.*, 2017, **56**, 8975–8985.
27 L. Abad Galán, A. N. Sobolev, B. W. Skelton, E. Zysman-Colman, M. I. Ogden and M. Massi, *Dalt. Trans.*, 2018, **47**, 12345–12352.
28 B. L. Reid, S. Stagni, J. M. Malicka, M. Cocchi, G. S. Hanan, M. I. Ogden and M. Massi, *Chem. Commun.*, 2014, **50**, 11580–11582.
29 L. Abad Galán, B. L. Reid, S. Stagni, A. N. Sobolev, B. W. Skelton, E. G. Moore, G. S. Hanan, E. Zysman-Colman, M. I. Ogden and M. Massi, *Dalt. Trans*, 2018, **47**, 7956–7964.
30 N. M. Shavaleev, R. Scopelliti, F. Gumy and J. C. G. Bünzli, *Inorg. Chem.*, 2009, **48**, 7937–7946.
31 Z. Ahmed and K. Iftikhar, *Polyhedron*, 2015, **85**, 570–592.
32 T. M. George, S. Varughese and M. L. P. Reddy, *RSC Adv.*, 2016, **6**, 69509–69520.
33 S. Biju, Y. K. Eom, J.-C. G. Bünzli and H. K. Kim, *J. Mater. Chem. C*, 2013, **1**, 6935.
34 P. Martín-Ramos, P. S. Pereira da Silva, V. Lavín, I. R. Martín, F. Lahoz, P. Chamorro-Posada, M. Ramos Silva and J. Martín-Gil, *Dalt. Trans.*, 2013, **42**, 13516.
35 K. Binnemans, *Coord. Chem. Rev.*, 2015, **295**, 1–45.
36 L. Yang, Z. Gong, D. Nie, B. Lou, Z. Bian, M. Guan, C. Huang, H. J. Lee and W. P. Baik, *New J. Chem.*, 2006, **30**, 791.
37 G. M. Sheldrick, *Acta Crystallogr. Sect. C-Struct. Chem.*, 2015, **71**, 3–8.
38 L. Abad Galán, A. N. Sobolev, E. Zysman-Colman, M. I. Ogden and M. Massi, *Dalt. Trans.*, 2018, Accepted Manuscript.
39 G. F. de Sá, O. L. Malta, C. de Mello Donegá, a. M. Simas, R. L. Longo, P. a. Santa-Cruz and E. F. da Silva, *Spectroscopic Properties and Design of Highly Luminescent Lanthanide Coordination Complexes*, 2000, vol. 196.
40 F. J. Steemers, W. Verboom, D. N. Reinhoudt, E. B. Vandertol and J. W. Verhoeven, *J. Am. Chem. Soc.*, 1995, **117**, 9408–9414.
41 Z. Ahmed, R. E. Aderne, J. Kai, H. I. P. Chavarria and M. Cremona, *Thin Solid Films*, 2016, **620**, 34–42.
42 Z. Zhang, C. Yu, L. Liu, H. Li, Y. He, X. Lü, W. K. Wong and R. A. Jones, *J. Photochem. Photobiol. A Chem.*, 2016, **314**, 104–113.
43 N. M. Shavaleev, R. Scopelliti, F. Gumy and J. C. G. Bünzli, *Eur. J. Inorg. Chem.*, 2008, **9**, 1523–1529.

DOI: 10.1039/C8DT04749A

Photophysical investigation of near infrared emitting lanthanoid complexes incorporating tris(2-naphthoyl)methane as a new antenna ligand

Laura Abad Galán, Satoshi Wada, Lee Cameron, Alexandre N. Sobolev, Yasuchika Hasegawa, Eli Zysman-Colman, Mark I. Ogden, and Massimiliano Massi

Study of a series of lanthanoid complexes reveals that ancillary ligands play a significant role in their photophysical properties.